

# THE MINIMUM MASS OF ROTATING MAIN SEQUENCE STARS AND ITS IMPACT ON THE NATURE OF EXTENDED MAIN SEQUENCE TURNOFFS IN INTERMEDIATE-AGE STAR CLUSTERS IN THE MAGELLANIC CLOUDS<sup>1</sup>

PAUL GOUDFROOIJ<sup>2</sup>, LÉO GIRARDI<sup>3</sup>, ANDREA BELLINI<sup>2</sup>, ALESSANDRO BRESSAN<sup>4</sup>, MATTEO CORRENTI<sup>2</sup>, AND GUGLIELMO COSTA<sup>4</sup>

<sup>2</sup> Space Telescope Science Institute, 3700 San Martin Drive, Baltimore, MD 21218, USA; [goudfroo@stsci.edu](mailto:goudfroo@stsci.edu), [bellini@stsci.edu](mailto:bellini@stsci.edu), [correnti@stsci.edu](mailto:correnti@stsci.edu)

<sup>3</sup> Osservatorio Astronomico di Padova – INAF, Vicolo dell’Osservatorio 5, I-35122 Padova, Italy; [leo.girardi@inaf.it](mailto:leo.girardi@inaf.it)

<sup>4</sup> SISSA, via Bonomea 365, I-34136 Trieste, Italy; [sbressan@sissa.it](mailto:sbressan@sissa.it), [gcosta@sissa.it](mailto:gcosta@sissa.it)

Received 2018 July 11; revised 2018 August 6; accepted 2018 August 11; published 2018 August 24

## ABSTRACT

Extended main sequence turn-offs (eMSTOs) are a common feature in color-magnitude diagrams (CMDs) of young and intermediate-age star clusters in the Magellanic Clouds. The nature of eMSTOs is still debated. The most popular scenarios are extended star formation and ranges of stellar rotation rates. Here we study implications of a kink feature in the main sequence (MS) of young star clusters in the Large Magellanic Cloud (LMC). This kink shows up very clearly in new *Hubble Space Telescope* observations of the 700-Myr-old cluster NGC 1831, and is located below the region in the CMD where multiple or wide MSes, which are known to occur in young clusters and thought to be due to varying rotation rates, merge together into a single MS. The kink occurs at an initial stellar mass of  $1.45 \pm 0.02 M_{\odot}$ ; we posit that it represents a lower limit to the mass below which the effects of rotation on the energy output of stars are rendered negligible at the metallicity of these clusters. Evaluating the positions of stars with this initial mass in CMDs of massive LMC star clusters with ages of  $\sim 1.7$  Gyr that feature wide eMSTOs, we find that such stars are located in a region where the eMSTO is already significantly wider than the MS below it. This strongly suggests that stellar rotation *cannot* fully explain the wide extent of eMSTOs in massive intermediate-age clusters in the Magellanic Clouds. A distribution of stellar ages still seems necessary to explain the eMSTO phenomenon.

**Keywords:** stars: rotation — globular clusters: individual (NGC 1783, NGC 1806, NGC 1831, NGC 1846, NGC 1866) — globular clusters: general — Magellanic Clouds

## 1. INTRODUCTION

One of the significant discoveries enabled by the high-precision photometry made possible with the Advanced Camera for Surveys (ACS) and the Wide Field Camera 3 (WFC3) onboard the *Hubble Space Telescope* (*HST*) was that of extended main sequence turnoffs (hereafter eMSTOs) in massive intermediate-age (1–2 Gyr old) star clusters in the Magellanic Clouds (Mackey & Broby Nielsen 2007; Milone et al. 2009; Goudfrooij et al. 2009). Such eMSTOs are much wider than the expectation of a simple stellar population (SSP) in conjunction with photometric uncertainties and stellar binarity. Furthermore, several eMSTO clusters feature a faint extension to the red clump of core helium burning giants, indicating the presence of a significant range of stellar core masses at the He flash (Girardi et al. 2009; Rubele et al. 2011).

The nature of the eMSTO phenomenon is still debated. The perhaps simplest explanation is an age spread of up to several  $10^8$  yr within these clusters (e.g., Mackey et al. 2008; Milone et al. 2009; Goudfrooij et al. 2014, 2015). In this “age spread” scenario, the shape of the star density distribution across the eMSTO is thought to reflect the combined effects of the histories of star formation and cluster mass loss due to strong cluster expansion following the death of massive stars in the central regions (Goudfrooij et al. 2014, hereafter G+14). Support in favor of this scenario was provided by G+14 by means of a correlation between MSTO width and central escape velocity, which is a proxy for the cluster’s ability to retain and/or accrete gas during its early evolution. G+14 also reported a

strong correlation between the fractional numbers of stars in the bluest region of the MSTO and those in the faint extension of the red clump, as expected from an age spread.

The leading alternative explanation of the eMSTO phenomenon is that it is caused by a spread of stellar rotation rates. Rotation lowers the luminosity and effective temperature at the stellar surface and Bastian & de Mink (2009) argued that this, when combined with projection effects, could cause eMSTOs similar to those observed. More recent studies revealed an opposite effect of stellar rotation, namely a longer main sequence (MS) lifetime due to internal mixing (Girardi et al. 2011; Georgy et al. 2014), thus mimicking a *younger* age. Significant support for the rotation scenario was provided by *HST* observations of younger clusters in the Large Magellanic Cloud (LMC) with ages of  $\sim 100$ –300 Myr (e.g., Correnti et al. 2015, 2017; Milone et al. 2015, 2017). These revealed the presence of eMSTOs combined with broadened or split MSes which are predicted to occur at these ages when a significant fraction of stars has rotation rates  $\Omega$  in excess of  $\sim 80\%$  of the critical rate ( $\Omega_C$ ) according to the Geneva SYCLIST isochrone models of Georgy et al. (2014), whereas it cannot easily be explained by age spreads (see D’Antona et al. 2015; Milone et al. 2016; Correnti et al. 2017). Finally, several stars in the MSTOs of young massive LMC clusters are now known to be strong H $\alpha$  emitters and thought to constitute equator-on Be stars that are rapidly rotating at  $\Omega/\Omega_C \gtrsim 0.5$  (Bastian et al. 2017; Correnti et al. 2017; Dupree et al. 2017; Milone et al. 2018).

These recent findings suggest that stellar rotation is part of the explanation of the eMSTO phenomenon (see also Mar-tocchia et al. 2018; Marino et al. 2018). However, there are relevant indications that other effects are at play as well. For

<sup>1</sup> Based on observations with the NASA/ESA *Hubble Space Telescope*, obtained at the Space Telescope Science Institute, which is operated by the Association of Universities for Research in Astronomy, Inc., under NASA contract NAS5-26555

example, the distributions of stars across the eMSTOs of several young massive clusters are *not* consistent with a coeval population of stars encompassing a range of rotation rates (as represented by the SYCLIST model predictions). Specifically, the number of stars on the “red” side of the MSTO is significantly higher than that expected if the “blue” side of the MSTO constitutes the bulk of the rotating stars in a coeval population of stars, hinting at the presence of an age spread in addition to rotation (see Correnti et al. 2017; Milone et al. 2016, 2017, 2018). Furthermore, Goudfrooij et al. (2017) showed that the distribution of stars across the eMSTOs of two massive LMC clusters with an age of  $\sim 1$  Gyr cannot be explained solely by a distribution of rotation rates according to the SYCLIST models, unless the orientations of rapidly rotating stars are heavily biased toward an equator-on configuration *in both clusters*, which is statistically highly improbable.

Finally, the SYCLIST isochrones only cover stellar masses  $M \geq 1.7 M_{\odot}$ , because this is the mass below which magnetic braking occurs due to the presence of a convective envelope, complicating the calculations of the influence of rotation to stellar evolutionary models. Notwithstanding this complexity, the magnetic braking for stars with  $M/M_{\odot} < 1.7$  is expected to decrease the effects of rotation, which should therefore result in MSTOs that get narrower with increasing age for intermediate-age LMC clusters with ages  $\gtrsim 1.2$  Gyr. However, this is inconsistent with observations in that the LMC clusters with the widest known MSTO’s have ages in the range 1.6 – 1.8 Gyr (see, e.g., G+14). These results cast doubt on the assertion that stellar rotation is the only cause of eMSTOs in intermediate-age clusters.

In the context of this debate, one may wonder if there might be model-independent features in the CMD that could yield a direct indication as to whether stellar rotation can fully explain the morphology of eMSTOs in massive intermediate-age clusters. In this paper, we study the implications of one such feature, namely an obvious kink in the MS of clusters younger than  $\approx 800$  Myr, which provides an empirical measurement of the stellar mass below which the influence of rotation to the width of the MS is negligible (for the metallicity of these clusters).

## 2. OBSERVATIONS AND DATA REDUCTION

Our attention to this kink in the MS of young LMC clusters was drawn by our recent *HST* observations of NGC 1831, which was the target of *HST* observing program GO-14688 (PI: P. Goudfrooij), using the UVIS channel of the Wide Field Camera 3 (hereafter WFC3/UVIS). Multiple dithered images were taken through the F336W and F814W filters, with total exposure times of 4180 s and 1480 s, respectively. Data analysis was carried out on the flat-fielded \*\_flc.fits images that were corrected for charge transfer inefficiency. Stellar photometry measurements were done with point spread function (PSF) fitting, using the “effective PSF” (ePSF) package for WFC3/UVIS (J. Anderson, private communication), which is based on the ePSF package for the ACS/WFC camera described in Anderson & King (2006). More details on this dataset and the photometry will be provided in a separate paper (M. Correnti et al., in preparation), but all data used in this paper can be obtained from MAST at <https://doi.org/10.17909/T9P41K>.

In order to minimize and illustrate the contamination by LMC field stars, we extract a circular “cluster region” containing the stars within a projected effective radius of the cluster center ( $r_e = 8.2$  arcsec, McLaughlin & van der Marel 2005).

For reference, we also extract a “background region” with the same area as the cluster region, but located near the edge of the image furthest away from the cluster center.

The CMD of NGC 1831 and the background region are shown in panel (a) of Figure 1. Note that the contamination by field stars is negligible. For comparison purposes, panel (b) of Figure 1 shows a CMD of a synthetic cluster based on a (non-rotating) PARSEC v1.2 isochrone (Bressan et al. 2012) with  $Z = 0.008$  and  $\log(\text{age/yr}) = 8.85$ . The simulation used a Salpeter (1955) initial mass function, a binary fraction of 0.2, and photometric uncertainties taken from the observations. Note that the MSTO of NGC 1831 is significantly more extended than the expectation of a SSP in conjunction with photometric uncertainties, as found for several other young and intermediate-age clusters in the LMC. While the morphology of the eMSTO and upper MS of NGC 1831 will be studied in detail in the context of the effects of stellar rotation in a separate paper (M. Correnti et al., in preparation), we focus here on the obvious kink in the MS of NGC 1831 at  $F814W \sim 21$ . Above this kink, the MS broadens into a fan-like shape which is likely due (at least in part) to a range of stellar rotation rates and rotation axis orientations in the cluster. Conversely, below this kink, the single-star MS emerges as narrow as would be expected for a SSP, while exhibiting a sharp curve downward in the  $F814W$  vs.  $F336W - F814W$  CMD which is not represented well by the isochrone model.

## 3. THE “KINK” IN THE MS OF YOUNG CLUSTERS

This MS kink is a general feature among young clusters in the LMC: Milone et al. (2018) studied  $F814W$  vs.  $F336W - F814W$  CMDs of 13 LMC clusters with ages between  $\sim 40$  Myr and 1.0 Gyr, and found that all of them feature an eMSTO along with an MS that is wide and/or split above a kink-like feature similar to that seen in NGC 1831. The narrow single-star MS emerging below this kink can also be seen in the CMDs by Milone et al. (2018), albeit typically at lower signal-to-noise ratio than in the CMD of NGC 1831 shown here. The exception to the latter is the case of NGC 1866, for which deep images were taken in programs GO-14204 (PI: A. P. Milone) and GO-14069 (PI: N. Bastian), which we downloaded from the *HST* archive and processed in the same way as that described above for NGC 1831. CMDs for NGC 1866 are shown in Figure 2.

To determine stellar parameters at the location of the MS kink, we compare the data of NGC 1831 and NGC 1866 with non-rotating PARSEC v1.2S isochrones. We fit the latter to the  $F814W$  vs.  $F336W - F814W$  CMDs above the MS kink in a way similar to Milone et al. (2018), i.e., interpreting the blue edge of the MS above the kink as the MS of non-rotating stars in these clusters, but now also taking the positions of the core-helium-burning stars into account. It can be seen in panel (a) of Figures 1 and 2 that this way of fitting isochrones to these CMDs results in non-optimal fits to the single-star MS below the kink in the sense that the isochrones indicate  $F336W - F814W$  colors redder than the data. However, the  $F814W$  vs.  $F555W - F814W$  CMD is actually fit very well by the same isochrones (above and below the MS kink), as can be seen for NGC 1866 in panel (b) of Figure 2. It therefore seems that the isochrones may have trouble describing the effective temperature of MS stars below this kink, possibly in conjunction with problems with the synthetic spectra used to convert the isochrones into colors involving passbands at shorter wavelengths, with adequate precision. This problem, which is discussed further below, is not restricted to the

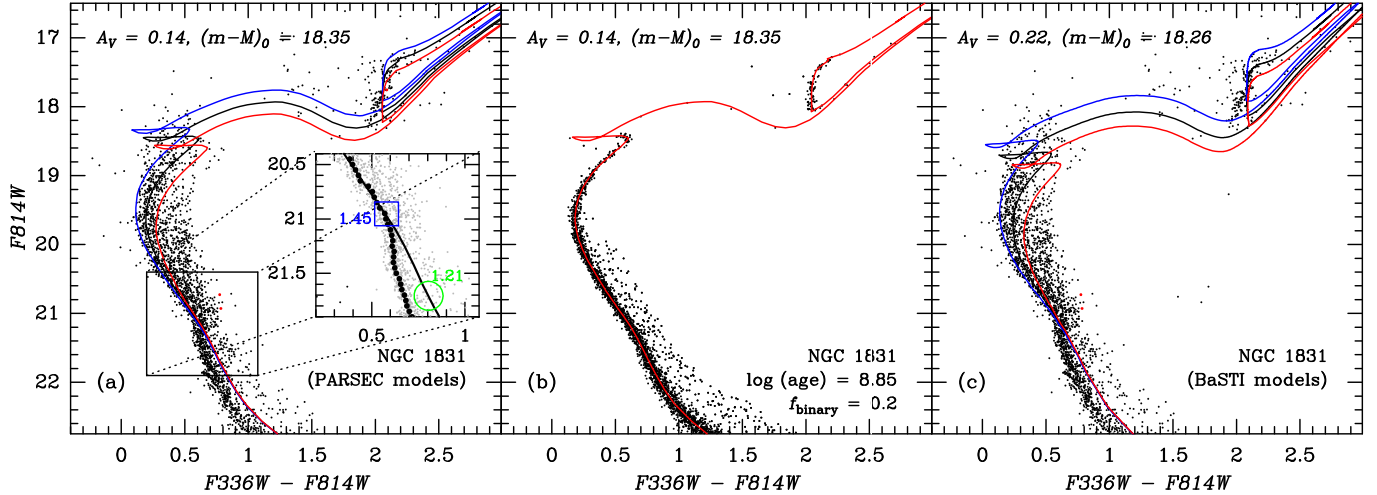


**Figure 1.** Panel (a):  $F814W$  vs.  $F336W - F814W$  CMD of NGC 1831 within its effective radius, along with PARSEC isochrones for  $Z = 0.008$  and  $\log(\text{age}/\text{yr}) = 8.80, 8.85$ , and  $8.90$  (in blue, black, and red, respectively). Values for  $A_V$  and  $(m-M)_0$  are indicated in the legend. The (very few) red dots indicate stars in the “background region” discussed in the text. Note the obvious “MS kink” at  $F814W \sim 21$ . The inset shows the kink region in which the individual stars are shown in grey, the black line is the PARSEC isochrone for  $\log(\text{age}/\text{yr}) = 8.85$ , and the black circles represent the MS fiducial as a function of  $F814W$  magnitude. The positions of stars with  $M/M_\odot = 1.45$  and  $1.21$  are highlighted using blue and green markers, respectively. Panel (b): Synthetic PARSEC cluster with  $Z = 0.008$ ,  $\log(\text{age}/\text{yr}) = 8.85$ , binary fraction of 0.2, and photometric uncertainties taken from the observations. Panel (c): Similar to panel (a), but now showing BaSTI isochrones for  $Z = 0.0057$  and ages of 0.6, 0.7, and 0.8 Gyr (in blue, black, and red, respectively).

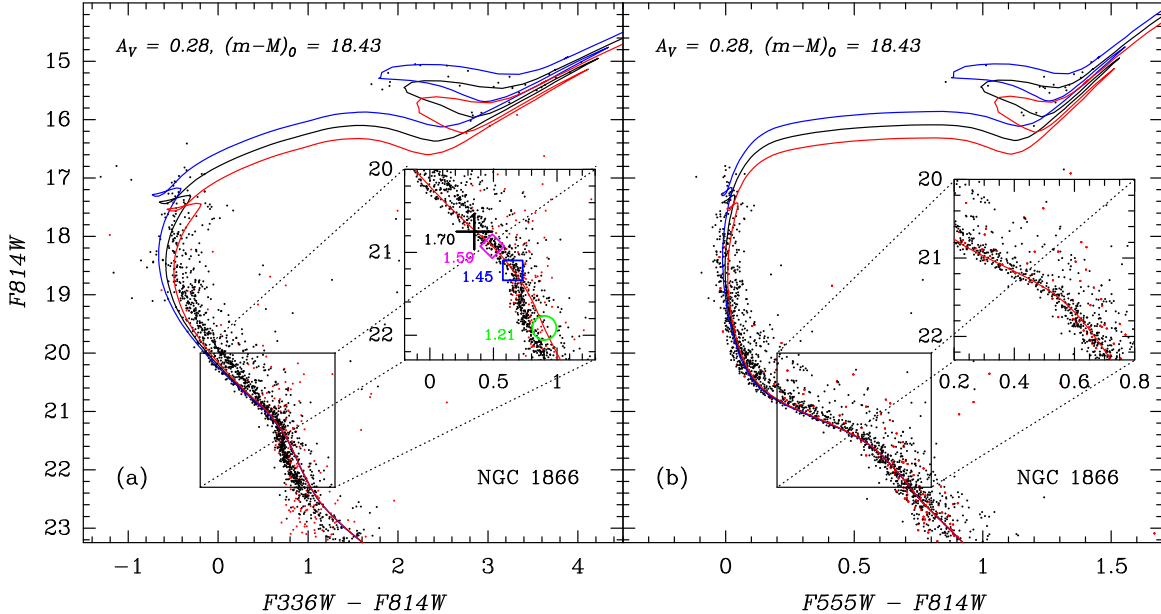


**Figure 2.** Panel (a): Similar to panel (a) of Figure 1, but now for NGC 1866. The PARSEC isochrones are for  $Z = 0.008$  and  $\log(\text{age}/\text{yr}) = 8.24, 8.30$ , and  $8.36$  in this case. The inset highlights the positions of stars with  $M/M_\odot = 1.70, 1.59, 1.45$ , and  $1.21$  using labels and markers in black (plus), magenta (diamond), blue (square), and green (circle), respectively. Panel (b): Similar to panel (a), but now using the  $F555W - F814W$  color. Note that the MS below the kink at  $F814W \sim 21.2$  is much better fit by the isochrones in  $F555W - F814W$  than in  $F336W - F814W$ . See discussion in Section 3.

PARSEC isochrone models which we use here as an example; several other popular models share the same issue. This is illustrated in panel (c) of Figure 1 for BaSTI (Pietrinferni et al. 2004) isochrones for which magnitudes were transformed to the *HST/WFC3* passbands following Goudfrooij et al. (2017).<sup>2</sup>

To determine the location of the kink, we construct MS fiducials that describe the peak of the  $F336W - F814W$  color distribution in the range  $20.5 \leq F814W \leq 22.0$ , using magnitude bins of 0.10 mag. The peak colors are taken to be

<sup>2</sup> We also verified this for the Geneva models (Mowlavi et al. 2012) as well as those of  $Y^2$  (Yi et al. 2001; Demarque et al. 2004), Dartmouth (Dotter et al. 2008) and MIST (Choi et al. 2016).

the maximum of their kernel density distributions, using an Epanechnikov kernel with adaptively chosen bandwidth (Silverman 1986). The kink brightness is then defined as the  $F814W$  magnitude beyond which the position of the MS fiducial in the CMD is systematically below that of the best-fitting isochrone. This is illustrated for NGC 1831 in the inset in Figure 1a where the kink is identified at  $F814W = 20.95 \pm 0.03$ . Using this method, and assuming the values of  $m - M$  and  $A_V$  shown in Figures 1 and 2, we find that the kink occurs at  $M_{F814W}^0 = 2.46 \pm 0.03$  and  $2.62 \pm 0.03$  for NGC 1831 and NGC 1866, respectively. Using linear interpolation within the isochrones, these luminosities correspond to initial stellar masses  $M/M_\odot = 1.45 \pm 0.02$  and  $1.45 \pm 0.02$ , respectively.

This mass is in the range where stellar structure undergoes significant changes between radiative and convective modes. Specifically, core convection is thought to occur for stars with  $M/M_{\odot} \gtrsim 1.3$  (e.g., Eggenberger et al. 2008), while stars with  $M/M_{\odot} \lesssim 1.7$  have convective envelopes, featuring magnetized winds which shed angular momentum that the star may have built up during its formation era (e.g., Georgy et al. 2014).

The shape and location of this MS kink, in conjunction with the fact that it is not well described by isochrone models, strongly suggests that its nature is related to the sudden onset of strong convection in the outer layers of stars with  $M \approx 1.45 M_{\odot}$ . In most isochrone models, the energy transport in the convection zone in stellar envelopes is modeled using the mixing-length theory (MLT) of Böhm-Vitense (1958), along with some degree of convective “overshoot” into the radiative region. In this theory, the mixing length  $\alpha$  is calibrated to fit the solar radius at the age of the Sun, which yields  $\alpha$  values of order 1.5 – 2.0 pressure scale heights. However, several pieces of evidence suggest that the efficiency of mixing varies significantly as a function of radius within stars. For example, the shape of Balmer line profiles of the Sun and lower-mass stars requires much smaller mixing lengths in the outer layers of stars ( $\alpha \sim 0.5$  rather than 1.5 – 2.0; see Fuhrmann et al. 1993). It was pointed out by Bernkopf (1998) that this discrepancy can be resolved by applying the full spectrum of turbulence (FST) convection model by Canuto & Mazzitelli (1991). D’Antona et al. (2002) compared model isochrones built with MLT and FST convection models and found that the FST model yields a sudden change in the MS slope at a location in the CMD that is very similar to that of the MS kink in NGC 1831, whereas the MLT model does not show this kink (see their Figure 2). As shown by D’Antona et al. (2002), this kink occurs at a stellar mass for which the convective envelope suddenly reaches much deeper into the interior than it does at a mass only 0.01  $M_{\odot}$  larger, thus causing a significant decrease of the temperature dependence of stellar mass,  $dT_{\text{eff}}/dM$ , with decreasing stellar mass. Since the  $T_{\text{eff}}$  at the MS kink is  $\sim 7800$  K, for which the stellar continuum peaks at  $\sim 3700$  Å according to Wien’s law, this sudden decrease of  $dT_{\text{eff}}/dM$  is measured most precisely using filters around that wavelength with a wide baseline, such as  $F336W - F814W$ ; conversely, red colors like  $F555W - F814W$  mainly measure the change in slope of the Rayleigh-Jeans tail of the spectrum, providing a less precise measure of  $T_{\text{eff}}$ .

We posit that the MS kink seen in NGC 1831 and the younger LMC clusters studied by Milone et al. (2018) and references therein is associated with this sudden change in the extent of the convective envelope at the metallicity of the young and intermediate-age LMC clusters. Furthermore, since the width of the single-star MS emerging down from the MS kink in NGC 1831 is fully consistent with a SSP, we posit that the kink also represents an empirical measure of the stellar mass below which rotation has no appreciable influence on the energy output of the star. This is consistent with the sudden increase of the depth of the convective envelope, given that the latter is believed to be the cause of magnetic braking of angular momentum in stars. Note that the stellar mass associated with this MS kink is formally a *lower limit* to the mass associated with the effective onset of stellar rotation, since the level of envelope convection needed to stifle the effects of rotation is not known theoretically. In this context, we note that the single-star MS of NGC 1866 is found to be narrowest at  $F814W = 20.95 \pm 0.05$ , corresponding to  $M = 1.59 \pm 0.03 M_{\odot}$  (see

inset in Figure 2a), which may turn out to be closer to the stellar mass associated with the effective onset of stellar rotation than the 1.45  $M_{\odot}$  mentioned above.

#### 4. COMPARISON WITH INTERMEDIATE-AGE EMSTO CLUSTERS

To illustrate the impact of the analysis in the previous section to the nature of eMSTO’s in intermediate-age clusters, we compare the high-quality *HST/ACS* photometry of NGC 1783, NGC 1806 and NGC 1846, three massive eMSTO clusters in the LMC with ages of  $\sim 1.7$  Gyr (Mackey et al. 2008; Milone et al. 2009; Goudfrooij et al. 2011), with the PARSEC isochrones (i.e., the same models as those used to determine the stellar mass at the MS kink in the previous section). These clusters were selected for this purpose because they feature the widest known eMSTOs among intermediate-age clusters in the LMC.<sup>3</sup> The *HST/ACS* photometry and the isochrone fitting procedure for these three clusters was described before by Goudfrooij et al. (2009, 2011). Figure 3 shows the  $F814W$  vs.  $F435W - F814W$  CMDs of these clusters along with three PARSEC isochrones for  $Z = 0.008$  and  $\log(\text{age/yr}) = 9.18, 9.24,$  and  $9.30$ , fitting the approximate blue end, center, and red end of the eMSTOs of these clusters, respectively. The locations of stars with the same initial mass as that associated with the MS kink in the younger LMC clusters, i.e.,  $M = 1.45 M_{\odot}$ , are shown as open squares on top of these isochrones. Note that *the widening of the eMSTOs in these clusters starts at significantly lower stellar masses than that associated with the MS kink in younger LMC clusters*. Specifically, the width of the single-star MS becomes consistent with a SSP at  $F814W \sim 21.5$  for these three intermediate-age clusters. This corresponds to an initial stellar mass of  $M = 1.21 \pm 0.02 M_{\odot}$ , where the uncertainty represents the dispersion of ages required to fit the distributions of stars across the MSTOs of these clusters as well as the different values of  $(m - M)_0$  and  $A_V$  of the three clusters. This initial mass is smaller by  $\sim 10\sigma$  than the initial mass associated with the MS kink in LMC clusters with ages  $\lesssim 700$  Myr, i.e., the location where their wide MS merges into a narrow single-star MS whose width is consistent with a SSP. This strongly suggests that stellar rotation is *not* the only cause of the extended MSTOs in the massive intermediate-age clusters.

#### 5. CONCLUSION

While several recent studies have provided important evidence in support of the stellar rotation scenario for the nature of eMSTOs in young clusters in the LMC, our results show that the very wide MSTOs in the most massive intermediate-age clusters with ages of 1.6 – 1.8 Gyr cannot fully be explained by rotation. This is simply because the MSTO in the latter clusters widens at a stellar mass well below that associated with the MS kink in younger clusters below which, as we showed above, the width of the MS of single stars is significantly narrower than that above the MS kink, and consistent with that of an SSP of non-rotating stars. These observations could be reconciled with the rotation-spread hypothesis only if there is a mass range in between 1.45 and 1.21  $M_{\odot}$  for which the effects of rotation take longer than 700 Myr (i.e., the age of NGC 1831) to produce a detectable effect at the stellar surface. Although the mixing induced by rotation could in principle produce effects that increase with age, it appears

<sup>3</sup> The widest known eMSTO is that of NGC 419 in the SMC (e.g., G+14), but we do not select that cluster for this comparison due to uncertainties associated with its significantly lower metallicity.

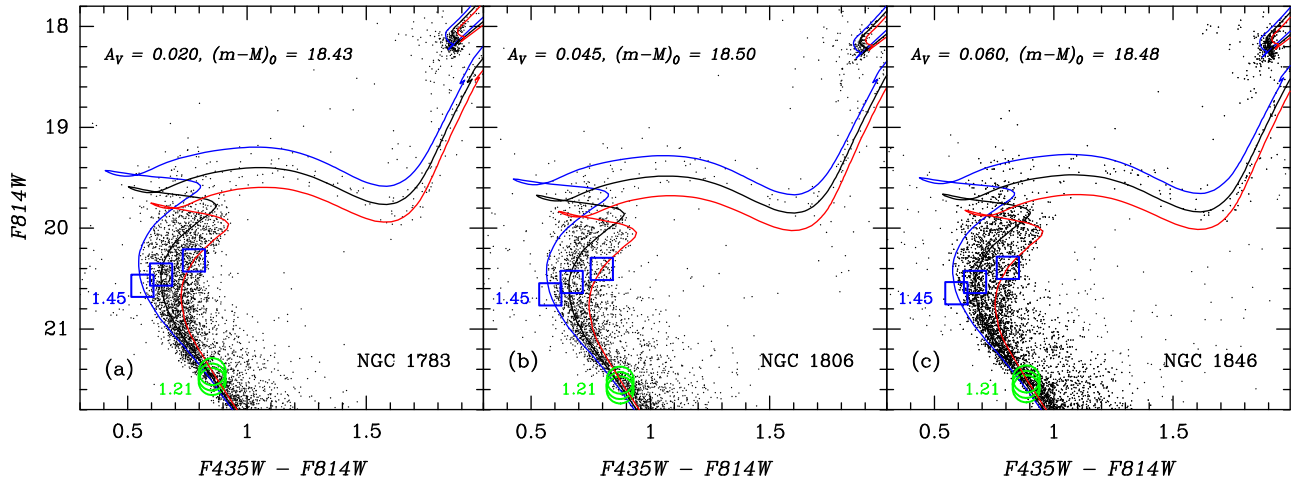


**Figure 3.** Panel (a): CMD of NGC 1783 within its core radius, taken from Goudfrooij et al. (2011), along with PARSEC isochrones for  $Z = 0.008$  and  $\log(\text{age/yr}) = 9.18, 9.24,$  and  $9.30$  (in blue, black, and red, respectively). Values for  $A_V$  and  $(m-M)_0$  are indicated in the legend. The open blue squares and open green circles indicate the positions of stars with  $M/M_\odot = 1.45$  and  $1.21$ , respectively, for each isochrone. Panel (b): similar to panel (a), but now for NGC 1806. Panel (c): similar to panel (a), but now for NGC 1846. See discussion in Section 4.

unlikely that they would manifest themselves so clearly at an age of  $\sim 1.7$  Gyr, also since magnetic braking is thought to be powerful in stars with strong envelope convection (i.e., with  $1.20 \lesssim M/M_\odot \lesssim 1.45$ ; see, e.g., van Saders et al. 2016).

This result constitutes new support for the age spread scenario on the nature of eMSTOs of massive intermediate-age clusters. Nevertheless, the recent studies of young clusters with eMSTOs have also clarified that rotation is part of the solution as well, so that the age spreads derived by G+14 are rendered overestimates (see discussion in Goudfrooij et al. 2017). Studies of the effects of rotation at  $M < 1.7 M_\odot$  are currently being pursued by different isochrone modelers including PARSEC and MIST, which should yield relevant new insights in this context.

We thank the referee for a constructive and helpful report which benefited the paper. Support for this project was provided by NASA through grants HST-GO-14688 and HST-AR-15023 from the Space Telescope Science Institute, which is operated by the Association of Universities for Research in Astronomy, Inc., under NASA contract NAS5-26555.

*Facilities:* HST(ACS, WFC3)

## REFERENCES

- Anderson, J., & King, I. R. 2006, Instrument Science Report ACS 2006-01 (Baltimore: STScI)
- Bastian, N., & de Mink, S. E. 2009, MNRAS, 398, L11
- Bastian, N., Cabrera-Ziri, I., Niederhofer, F., et al. 2017, MNRAS, 465, 4795
- Bernkopf, J. 1998, A&A, 332, 127
- Böhm-Vitense, E. 1958, Z. Astroph. 46, 108
- Bressan, A., Marigo, P., Girardi, L., et al. 2012, MNRAS, 427, 127
- Canuto, V. M., & Mazzitelli, I. 1991, ApJ, 370, 295
- Choi, J., Dotter, A., Conroy, C., et al. 2016, ApJ, 823, 102
- Correnti, M., Goudfrooij, P., Kalirai, J. S., et al. 2014, ApJ, 793, 121
- Correnti, M., Goudfrooij, P., Puzia, T. H., & de Mink, S. E. 2015, MNRAS, 450, 3054
- Correnti, M., Goudfrooij, P., Bellini, A., Kalirai, J. S., & Puzia, T. H. 2017, MNRAS, 467, 3628
- D’Antona, F., Montalbán, J., Kupka, F., & Heiter, U. 2002, ApJL, 564, L93
- D’Antona, F., Di Criscienzo, M., Decressin, T., et al. 2015, MNRAS, 453, 2637
- Demarque, P., Woo, J.-H., Kim, Y.-C., & Yi, S. K. 2004, ApJS, 155, 667
- Dotter, A., Chaboyer, B., Jevremović, D., et al. 2008, ApJS, 178, 89
- Dupree, A. K., Dotter, A., Johnson, C. I., et al. 2017, ApJL, 846, L1
- Eggenberger, P., Meynet, G., Maeder, A., et al. 2008, Ap&SS, 316, 43
- Fuhrmann, K., Axer, M., & Gehren, T. 1993, A&A, 271, 451
- Georgy, C., Granada, A., Ekström, S., et al. 2014, A&A, 566, A21
- Girardi, L., Rubele, S., & Kerber, L. 2009, MNRAS, 394, L74
- Girardi, L., Eggenberger, P., & Miglio, A. 2011, MNRAS, 412, L103
- Goudfrooij, P., Puzia, T. H., Kozhurina-Platais, V., & Chandar, R. 2009, AJ, 137, 4988
- Goudfrooij, P., Puzia, T. H., Kozhurina-Platais, V., & Chandar, R. 2011, ApJ, 737, 3
- Goudfrooij, P., Girardi, L., Kozhurina-Platais, V., et al. 2014, ApJ, 797, 35 (G+14)
- Goudfrooij, P., Girardi, L., Rosenfield, P., et al. 2015, MNRAS, 450, 1693
- Goudfrooij, P., Girardi, L., & Correnti, M. 2017, ApJ, 846, 22
- Mackey, A. D., & Broby Nielsen, P. 2007, MNRAS, 379, 151
- Mackey, A. D., Broby Nielsen, P., Ferguson, A. M. N., & Richardson, J. C. 2008, ApJ, 681, L17
- Marino, A. F., Milone, A. P., Casagrande, L., et al. 2018, submitted to ApJ (arXiv:1807.05888)
- Martocchia, S., Niederhofer, F., Dalessandro, E., et al. 2018, MNRAS, 477, 4696
- McLaughlin, D. E., & van der Marel, R. P. 2005, ApJS, 161, 304
- Milone, A. P., Bedin, L. R., Piotto, G., & Anderson, J. 2009, A&A, 497, 755
- Milone, A. P., Bedin, L. R., Piotto, G., et al. 2015, MNRAS, 450, 3750
- Milone, A. P., Marino, A. F., D’Antona, F., et al. 2016, MNRAS, 458, 4368
- Milone, A. P., Marino, A. F., D’Antona, F., et al. 2017, MNRAS, 465, 4363
- Milone, A. P., Marino, A. F., Di Criscienzo, M., et al. 2018, MNRAS, 477, 2640
- Mowlavi, N., Eggenberger, P., Meynet, G., et al. 2012, A&A, 541, A41
- Pietrinferni, A., Cassisi, S., Salaris, M., & Castelli, F. 2004, ApJ, 612, 168
- Rubele, S., Girardi, L., Kozhurina-Platais, V., Goudfrooij, P., & Kerber, L. 2011, MNRAS, 414, 2204
- Rubele, S., Girardi, L., Kozhurina-Platais, V., et al. 2013, MNRAS, 433, 2774
- Salpeter, E. E. 1955, ApJ, 121, 161
- Silverman, B. W. 1986, in *Density Estimation for Statistics and Data Analysis*, Chap and Hall/CRC Press, Inc.
- van Saders, J. L., Ceillier, T., Metcalfe, T. S., et al. 2016, Nature, 529, 181
- Yi, S. K., Demarque, P., Kim, Y.-C., et al. 2001, ApJS, 136, 417